2.3 Review of Iodine-129 Source Term

The historical I-129 source term at the INTEC is described in Chapters 5 and 6 of Appendix F of the WAG-3 OU 3-13 RI/BRA report (DOE-ID, 1997). For the RI/BRA study, the INTEC releases were defined as one of three types: (1) known releases, (2) service waste releases, or (3) soil contamination releases. The contaminant sources evaluated in the OU 3-13 study are listed below.

Known releases - The I-129 from known releases were assumed to come from accidental liquid releases in the Tank Farm area. There have been three major releases identified. They are defined as the CPP-28, CPP-31, and 1986 releases.

- It was assumed that the CPP-31 and the 1986 releases contained I-129. The CPP-31 release occurred over 30 days during the month of November, 1972.
- 1986 release occurred over 26 days during the month of July, 1986.
- The CPP-28 release occurred over the period of 1956 through 1974, however, it was assumed not to contain I-129. This is clearly not true, however, as will be shown later, the estimated inventory of I-129 disposed to the injection well is far larger than that released at the Tank Farm, therefore, this source omission was assumed to be insignificant.

Service Waste Releases - There were two primary service waste releases.

- Injection well - This well was drilled to discharge the service waste water directly to the aquifer. The injection well operated from 1953 through 1986. During the period of Jan. 1968 - Sep. 1970, the well casing corroded and collapsed, discharging the service wastewater directly to the vadose zone.
- Service Waste Ponds (SWPs) - These ponds were constructed to replace the injection well. A portion of the service waste water was discharged to the ponds starting in 1984 and all the service waste water has been discharged to the ponds since 1986.

Soil Contamination Releases - Soil contaminated with I-129 throughout the INTEC area was assumed to be available in 1992 for transport through the vadose zone to the aquifer.

The flux of I-129 to the aquifer was estimated based on service waste disposal records for the injection well. For the other sources, a vadose zone flow and transport numerical model was used to calculate the I-129 flux to the aquifer. Figures 2-10 and 2-11 show the I-129 flux to the aquifer from the injection well and to the vadose zone when the injection well failed. Figure 2-12 shows the I-129 flux to the aquifer predicted by the vadose zone model from the vadose zone sources. The simulated flux in Figure 2-12 includes the I-129 from the injection well that was discharged to the vadose zone during the periods when the injection well failed (shown in Figure 2-11), as well as the I-129 from the known releases and soil contamination.

As shown in Figure 2-10, the injection well flux to the aquifer was assumed to be a relatively constant 1.2e-8 pCi/d for approximately 20 years. A similar flux to the vadose zone is shown in Figure 2-11 when the injection well failed. In Figure 2-12, the flux to the aquifer shows a sharp rise to about 3.5e+7 pCi/d when the injection well fails, after which, the flux falls off to approximately 1e+7 pCi/d for the next 50 years. The daily flux during the years of direct injection to the aquifer is significantly higher than the simulated flux from the vadose zone.

Table 2-2 is a summary of the I-129 sources assumed in the OU 3-13 RI/BRA report (DOE-ID, 1997) and each source is explained in greater detail below.

- The I-129 source from the Tank Farm releases is based on estimates of the liquid release volumes and the average I-129 concentrations in the liquid release. The I-129 contribution from the Tank Farm is essentially zero (0.5% of the total).
- The I-129 source from the injection well is significantly larger than the other sources accounting for 91.5% of the total I-129 source to the aquifer. The injection well source term was estimated from data in the RWMIS database. Data was available for the period May 1976 through April 1985. It was assumed that the average I-129 flux during this period is representative of the entire period of injection well operation.
- The I-129 source from the SWPs is approximately 5.4% of the total I-129 source to the aquifer. It was assumed that all of the I-129 from the SWP was in the SWP disposals between 1984 through 1990. After 1990, the SWP water was assumed to have no I-129.
- The I-129 source from the soil contamination was calculated to be approximately 2.5% of the total I-129 source to the aquifer. Although all of the I-129 in the soil was assumed to be available for transport at the same time (January 1992), the I-129 is distributed across the INTEC facility and the leaching water will be diluted and the I-129 dispersed as it moves through the vadose zone. Therefore, the I-129 soil contamination had little influence on the I-129 concentrations in the aquifer.

Table 2-2 Summary of the I-129 sources and time frame of environmental and aquifer flux. (From Table 5-42 in the Appendix F of the OU 3-13 RI/BRA, DOE-ID, 1997).

I-129 Source	Source Activity		Primary Time Frame	
	Total (Ci)	% of Total	Flux to Vadose Zone	Flux to Aquifer
Tank Farm	0.007	0.5%	11/1/72-11/30/72	No aquifer flux
Injection Well	1.39	91.6%	1/68 - 9/70*	1/53 - 12/67 10/70 - 3/86
SWPs	0.08	5.4%	4/84 - 1/90	No aquifer flux
Soil Contamination	0.04	2.6%	1/92	No aquifer flux
* Injection well collapse resulting in deep vadose zone contamination.				

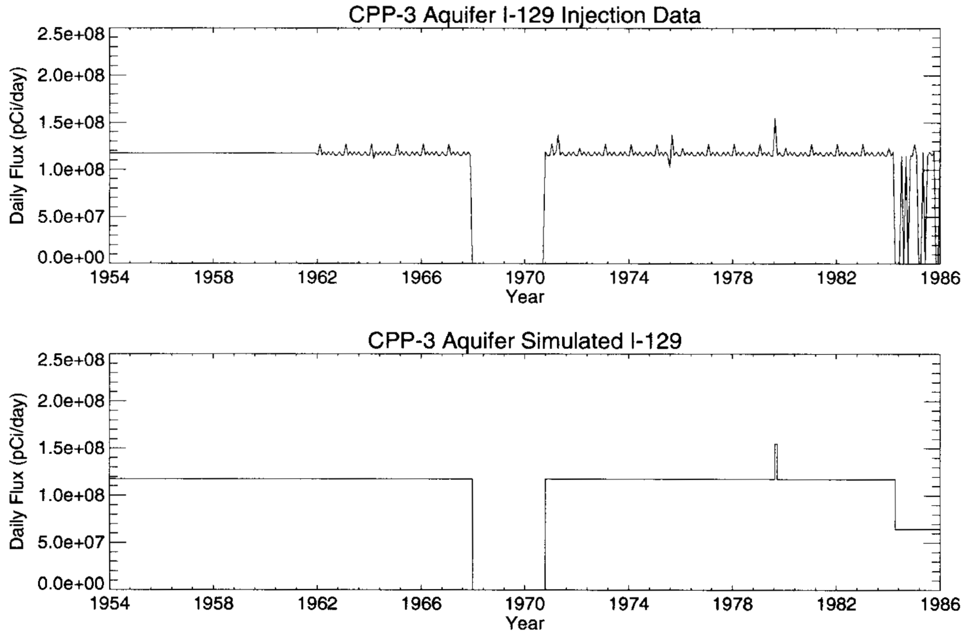

Figure 2-10 I-129 actual and simulated disposal history to the aquifer from the CPP-3 injection well.

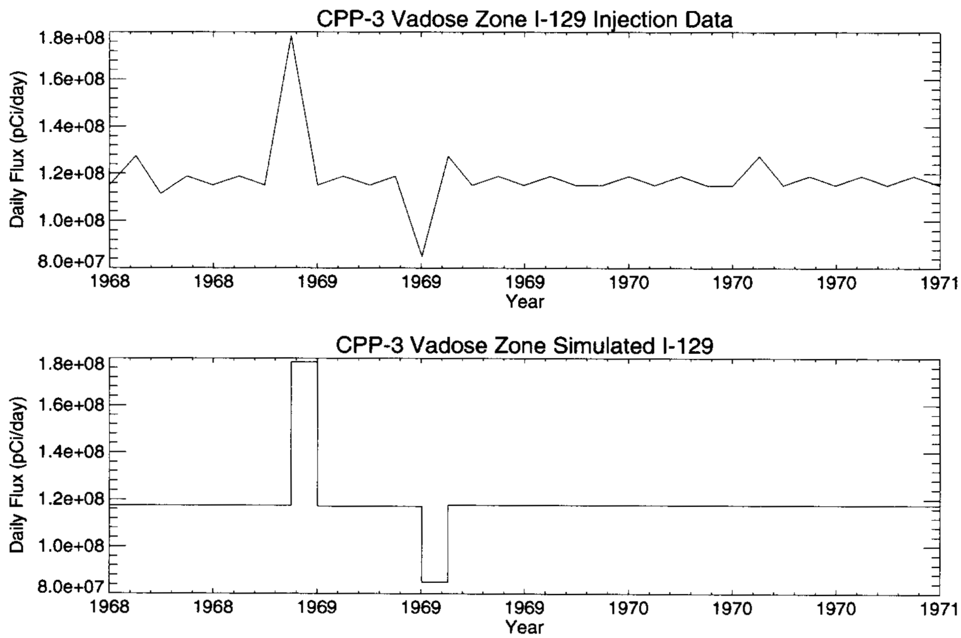

Figure 2-11 I-129 actual and simulated disposal history to the vadose zone from the CPP-3 injection well.

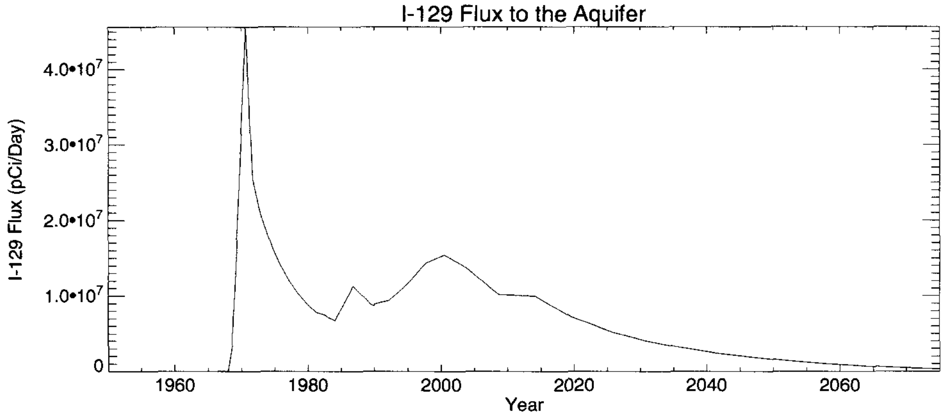

Figure 2-12 I-129 simulated mass flux from the vadose zone.

2.4 Review of OU 3-13 RI/BRA Iodine-129 Simulation Results

The OU 3-13 RI/BRA modeling predicted a relatively large area of the Snake River Plain Aquifer will have I-129 concentrations greater than the 1 pCi/L MCL in the year 2095. Two areas of the HI interbed contained I-129 at concentrations above the MCL in 2095. The first area is immediately southwest of the INTEC and has a peak concentration of 3.0 pCi/L. The second area is west of Lincoln Boulevard and north of State Highway 20 and has a peak concentration of 1.4 pCi/L. All grid blocks with concentrations over 1pCi/L are located within the HI interbed.

These values are different from those presented in Appendix F of the OU 3-13 RI/FS. The Appendix F peak was 4.7 pCi/L. The difference is due to a coding error in TETRAD version 12.2. All the RI/BRA fate and transport simulations were performed from a common set of initial conditions, which were read from a restart file. The restart file option in TETRAD allows a simulation to be stopped and restarted at any time without a loss of simulation information. However in TETRAD version 12.2, different simulation results were obtained when the simulation was run with and without stopping the simulation after initial conditions were obtained. TETRAD version 12.7 was used to verify the OU 3-13 simulations and identical results were obtained with or without using the restart option. Figures 2-13 through 2-22 presents a layer by layer comparison of TETRAD version 12.2 and 12.7 simulation results for 5 times (1959, 1972, 1992, 2025, and 2095). The version 12.7 results plotted in red over the version 12.2 results in black. A summary of peak I-129 concentration in each layer at the 5 times is provided in Table 2-3.

The TETRAD coding error in version 12.2 is due to TETRAD failing to maintain the specified dispersivity value. Upon a restart, the TETRAD code reset the simulation dispersivity value to 0m from the specified 5 m value. As can be seen in Figures 2-13 through 2-22 and Table 2-3, the peak concentrations between the two versions 12.2 and 12.7 are initially very similar. However as simulation time progresses, the attenuation from the specified dispersion increasingly lowers the simulated peak value in each layer.For comparison. The differences between TETRAD version 12.2 and 12.7 are provided in Appendix C-1.

Figure 2-23 illustrates the plume axis as predicted by the RI/BRA model in year 2000 and 2095. Figures 2-24 and 2-25 illustrate a vertical cross sections of the rediscretized model's plume axis for the years 1954, 1965, 1981, 2000, 2025, 2058, 2074 and 2095. The 0.01, 0.1, and 1.0pCi/L isopleths are illustrated by a thin dashed, thin, and thick black lines, respectively. The aquifer bottom is shown as a thick red line and the HI interbed is denoted by dashed lines. The CPP-3 injection well was simulated as a fully screened well extending 40 m below the water table and is shown in Figures 2-24 and 2-25 as a vertical blue line in the upper left corner of each cross-section. The CPP-03 injection well is screened across the HI interbed, which is present approximately 25 m below the water table. I-129 disposal begins in 1954 and by 1965, the down gradient migration of I-129 in the HI interbed lags behind that in the surrounding basalt. However in the year 2058, clean water movement through the contamination area lags in the interbed and isolated high concentrations of I-129 persist in the interbed where aquifer velocity is low.

Table 2-3 Maximum I-129 concentrations predicted with TETRAD version 12.2 and 12.7.

	Maximum I-129 Concentration (pCi/L)									
	5/1959		11/1972		4/1992		3/2025		10/2095	
Layer	TETRAD Version 12.2	TETRAD Version 12.7	TETRAD Version 12.2	TETRAD Version 12.7	TETRAD Version 12.2	TETRAD Version 12.7	TETRAD Version 12.2	TETRAD Version 12.7	TETRAD Version 12.2	TETRAD Version 12.7
1	28.2	28.1	22.9	22.8	4.6	4.6	2.6	2.6	0.3	0.3
2	33.4	33.2	31.8	31.2	4.8	4.8	2.4	2.4	0.4	0.3
3	35.3	35.5	31.9	32.1	7.0	6.8	1.8	1.8	1.3	0.9
4	22.9	22.6	16.7	16.6	14.3	13.2	5.7	4.9	1.2	1.7
5	32.5	32.3	30.0	29.8	13.7	13.4	9.0	8.4	4.7	3.0
6	32.8	32.8	30.4	30.4	14.3	13.2	7.2	5.7	2.8	1.5
7	33.0	33.0	30.4	30.4	11.8	10.1	4.2	3.3	1.1	1.1
8	31.8	31.6	29.5	29.3	10.3	10.1	4.2	3.5	1.5	1.4
9	30.0	29.7	28.1	27.7	12.2	12.1	4.5	4.3	1.3	1.1
10	26.7	26.5	23.8	23.5	13.2	13.0	5.8	5.5	0.4	0.4
Maximum for All Layers	35.3	35.5	31.9	32.1	14.3	13.2	9.0	8.4	4.7	3.0

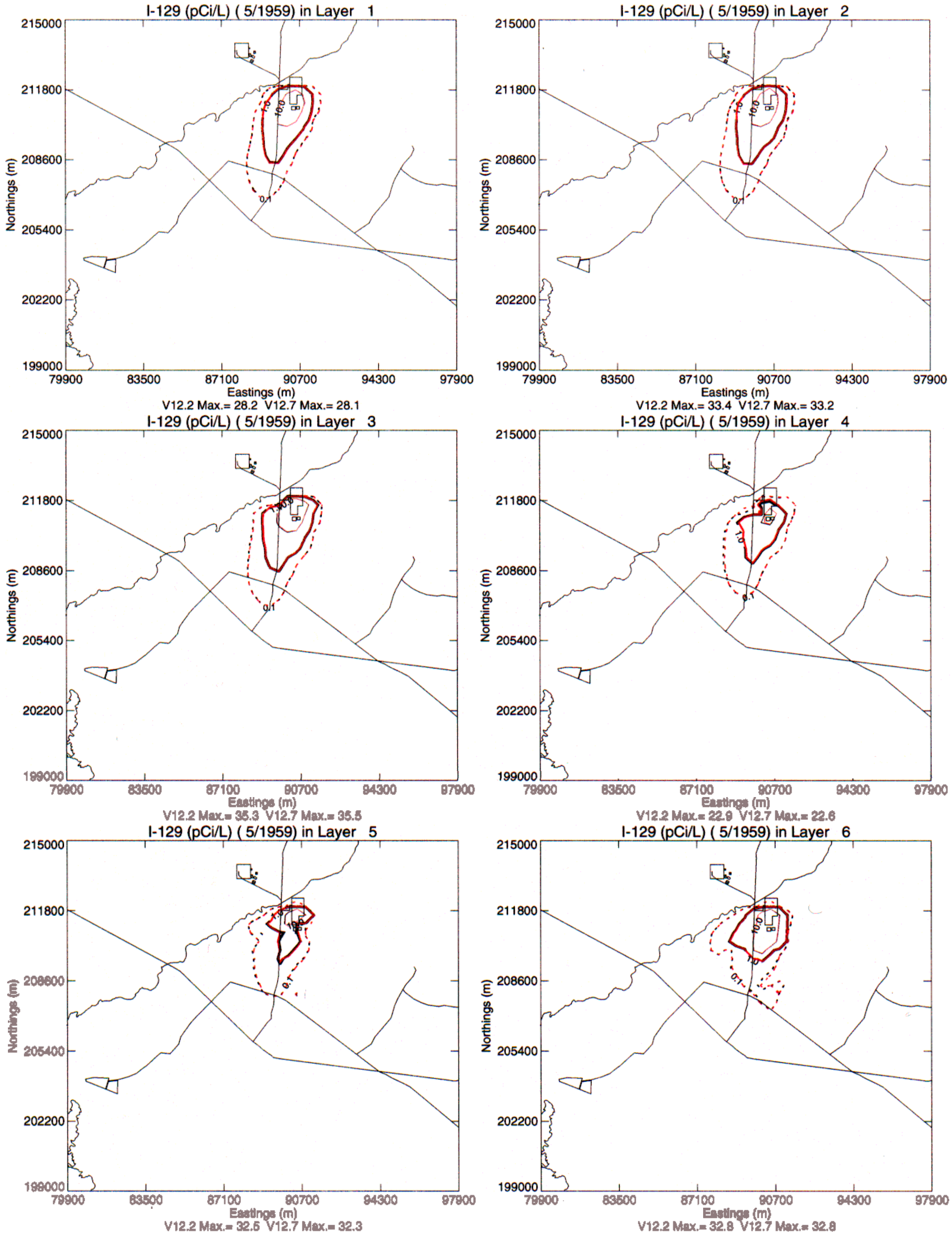

Figure 2-13 RI/BRA model I-129 concentrations, TETRAD version 12.2 (black) vs. 12.7 (red) for layers 1-6 in 5/1959.

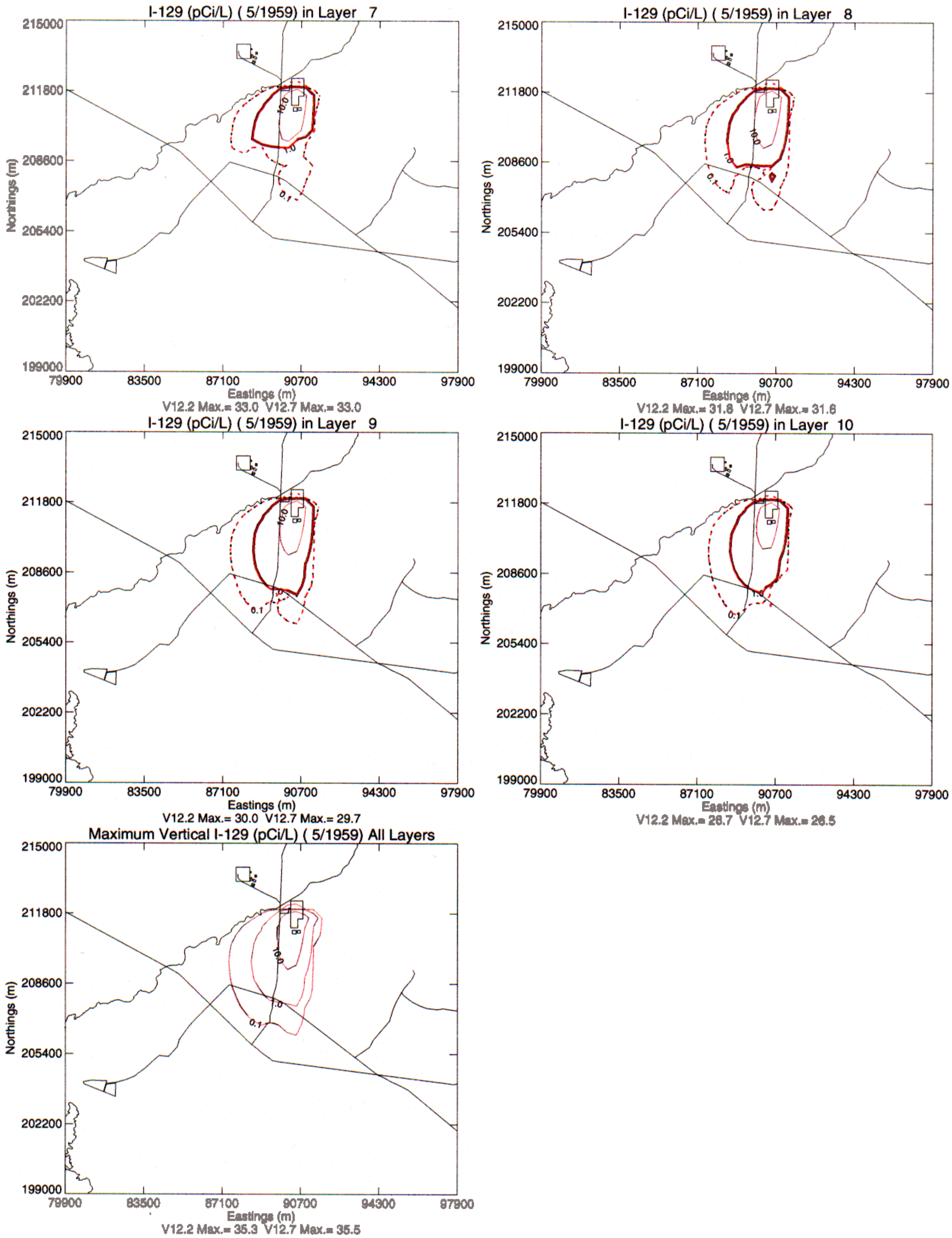

Figure 2-14 RI/BRA model I-129 concentrations, TETRAD version 12.2 (black) vs. 12.7 (red) for layers 7-10 in 5/1959.

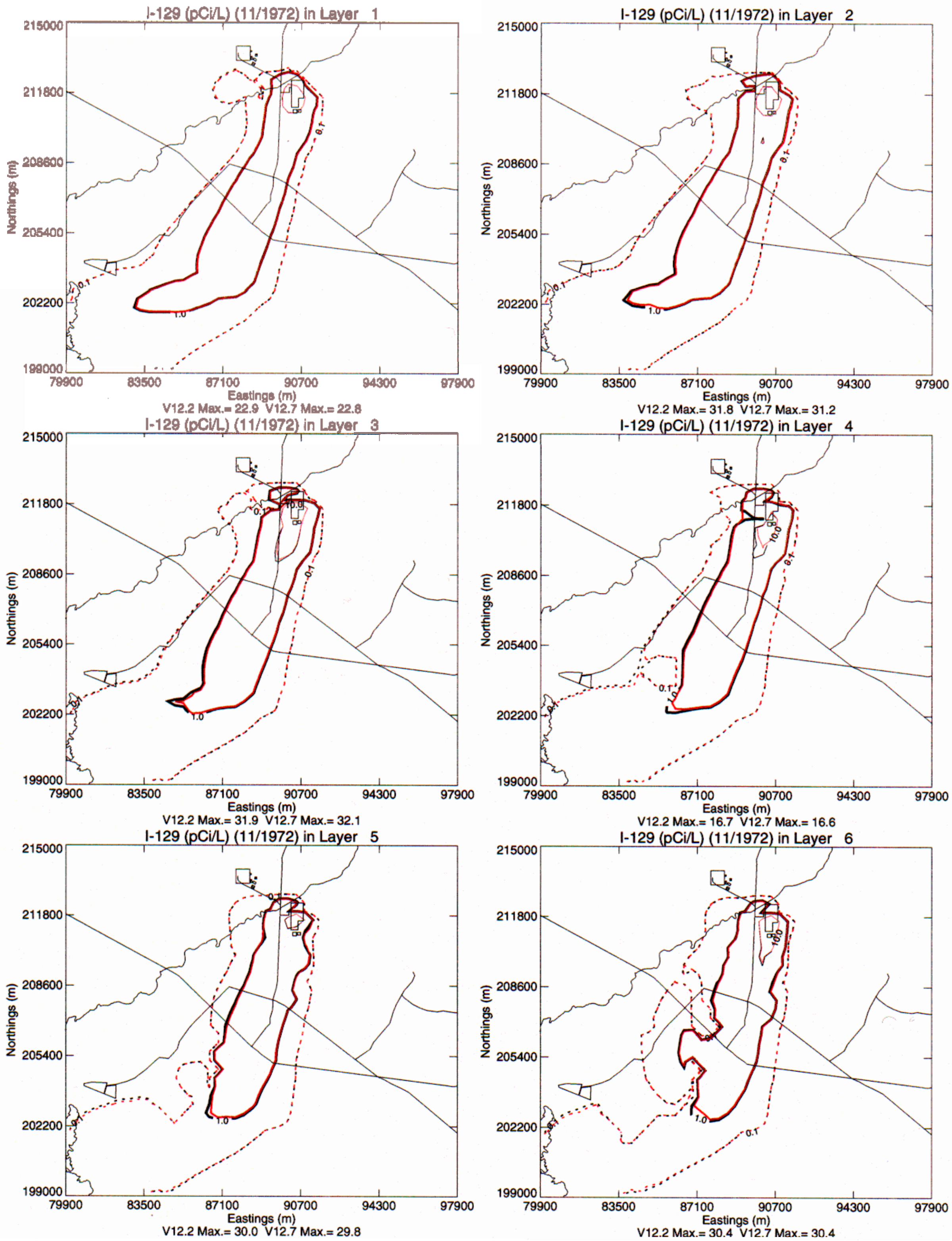

Figure 2-15 RI/BRA model I-129 concentrations, TETRAD version 12.2 (black) vs. 12.7 (red) for layers 1-6 in 11/1972.

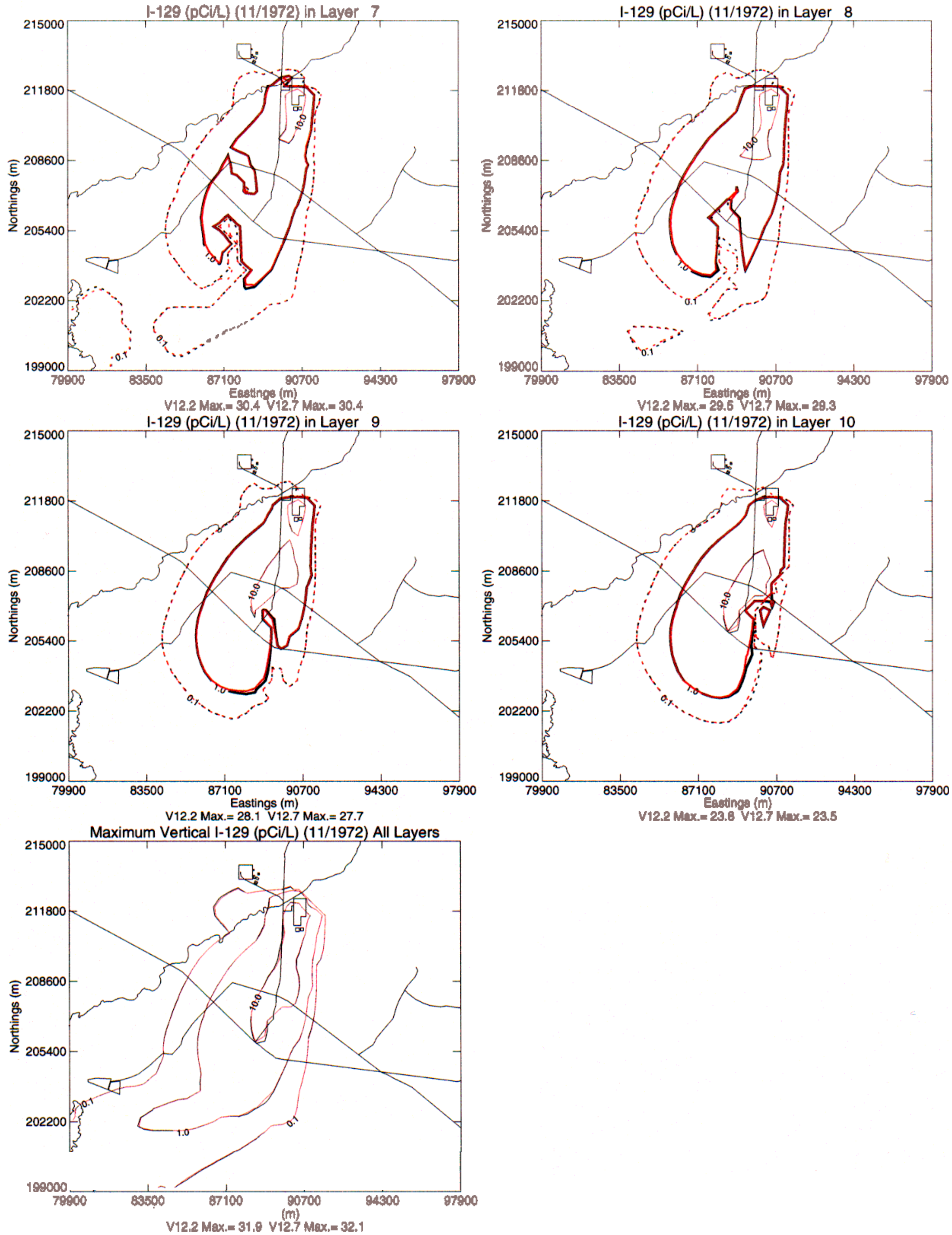

Figure 2-16 RI/BRA model I-129 concentrations, TETRAD version 12.2 (black) vs. 12.7 (red) for layers 7-10 in 11/1972.

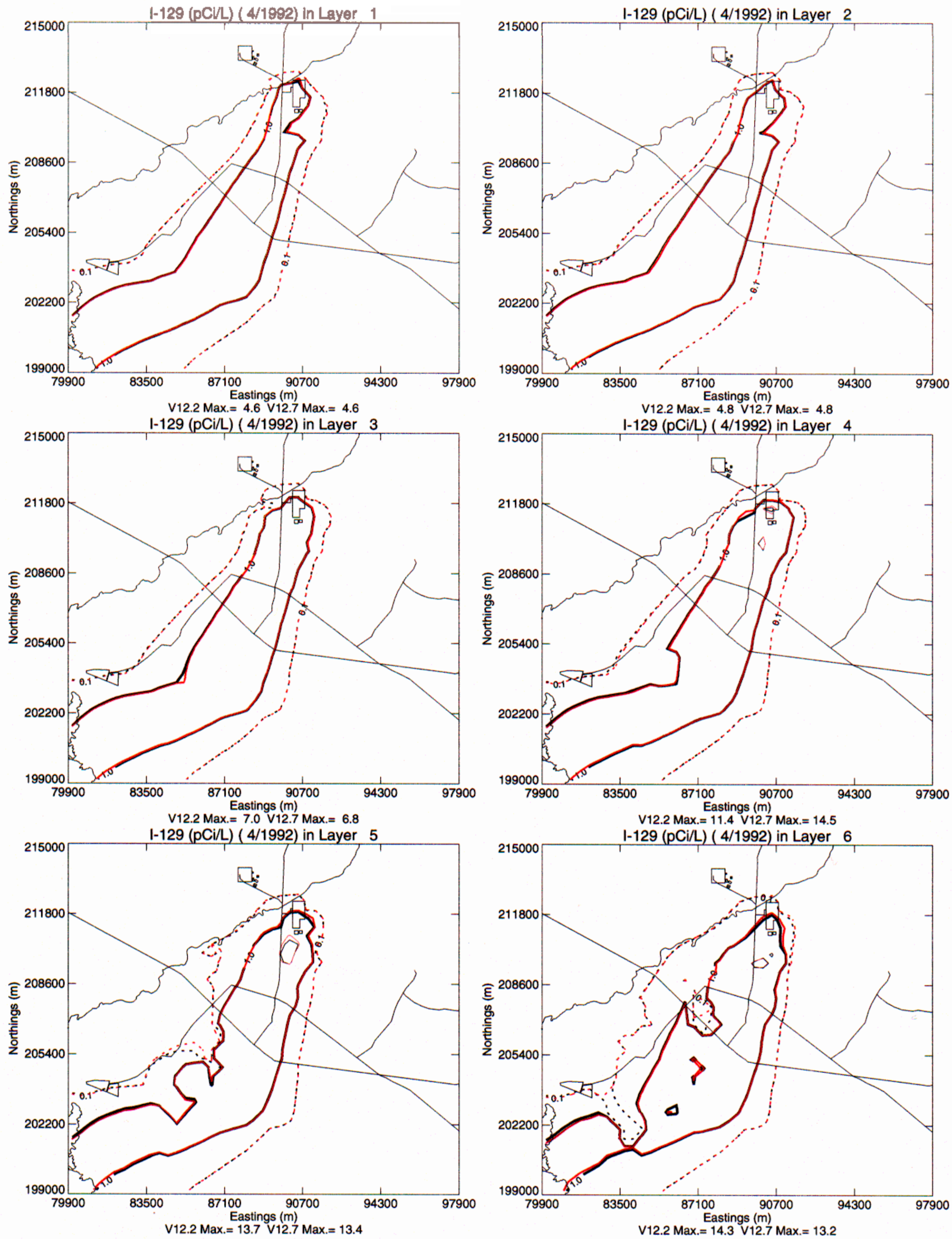

Figure 2-17 RI/BRA model I-129 concentrations, TETRAD version 12.2 (black) vs. 12.7 (red) for layers 1-6 in 4/1992.

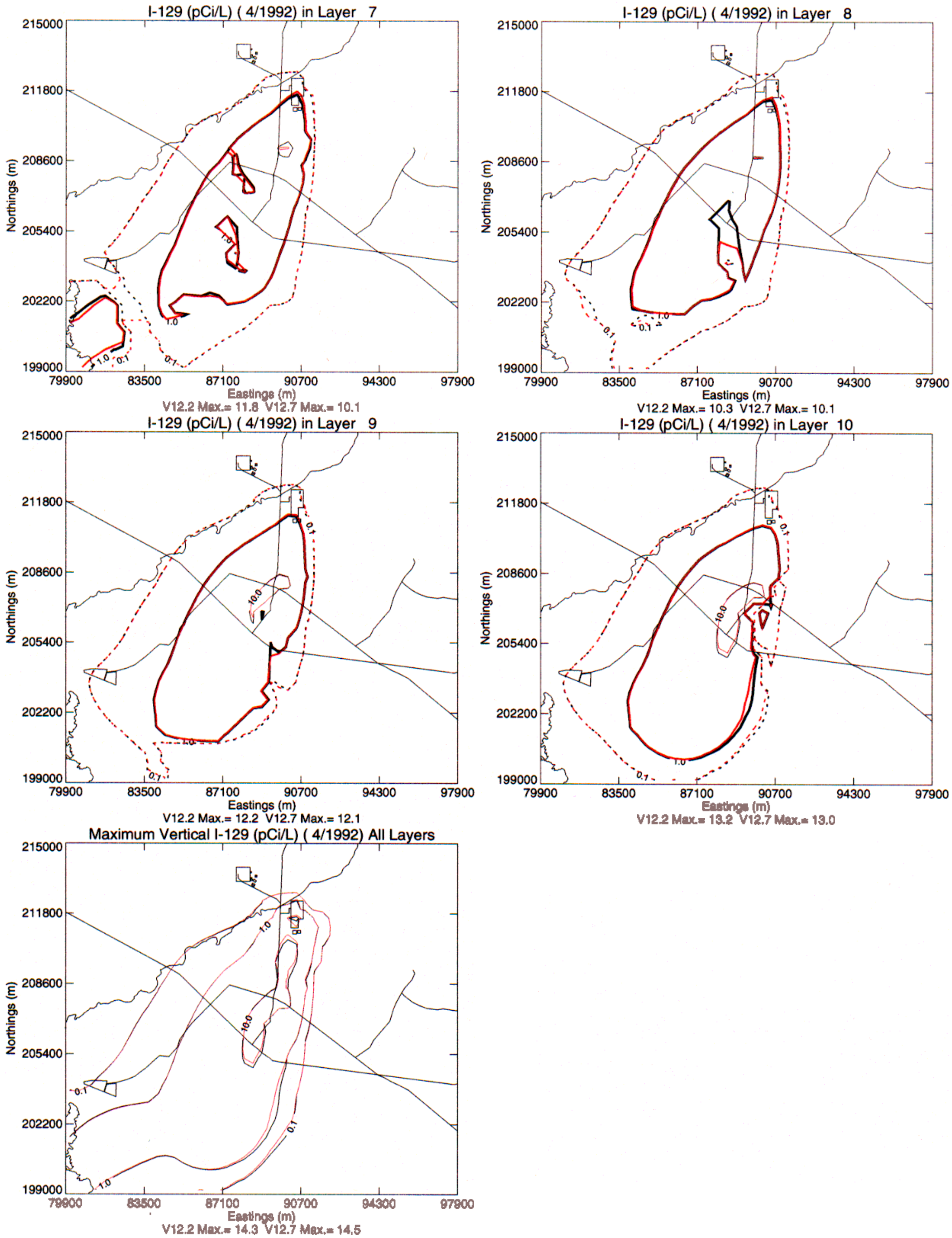

Figure 2-18 RI/BRA model I-129 concentrations, TETRAD version 12.2 (black) vs. 12.7 (red) for layers 7-10 in 4/1992.

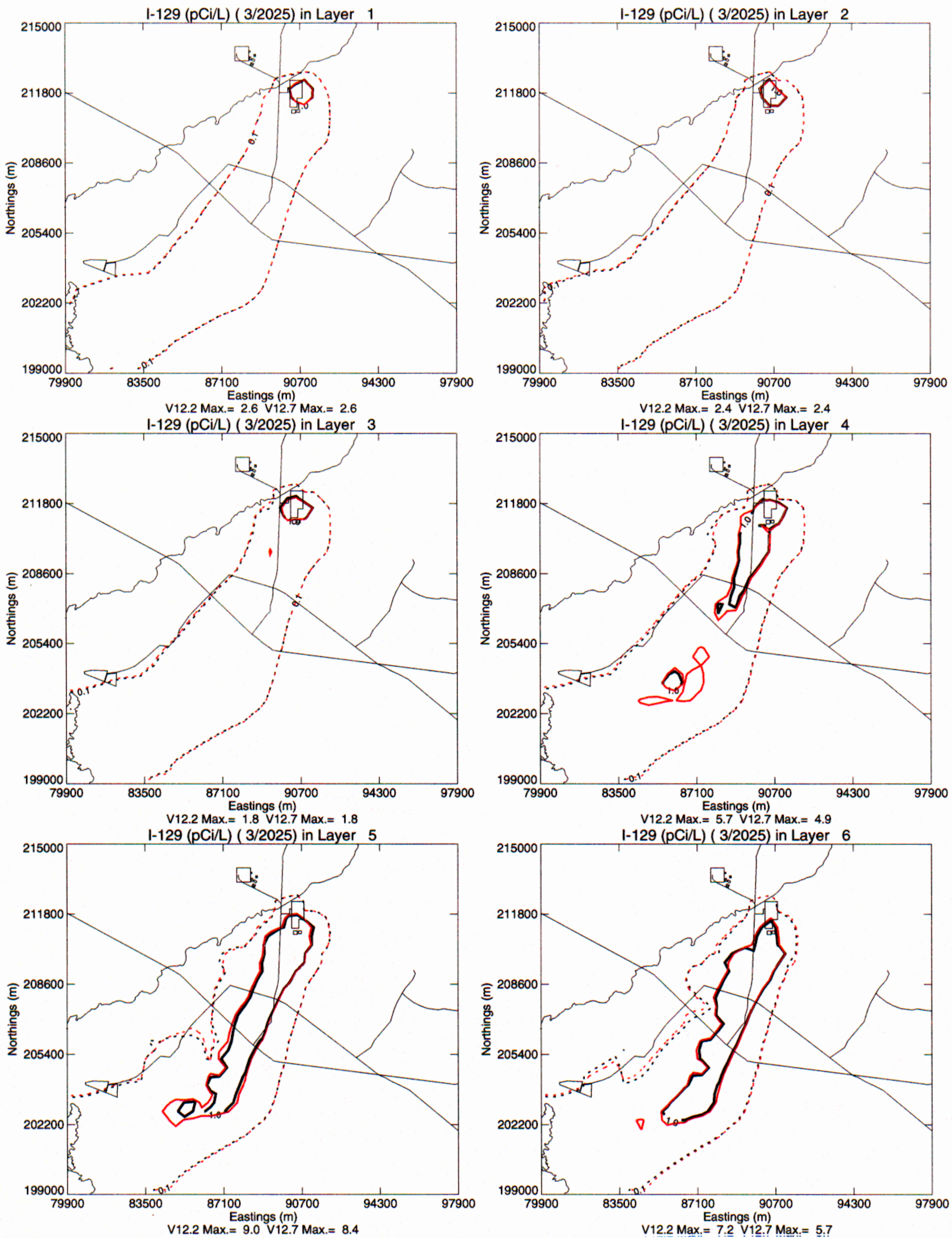

Figure 2-19 RI/BRA model I-129 concentrations, TETRAD version 12.2 (black) vs. 12.7 (red) for layers 1-6 in 3/2025.

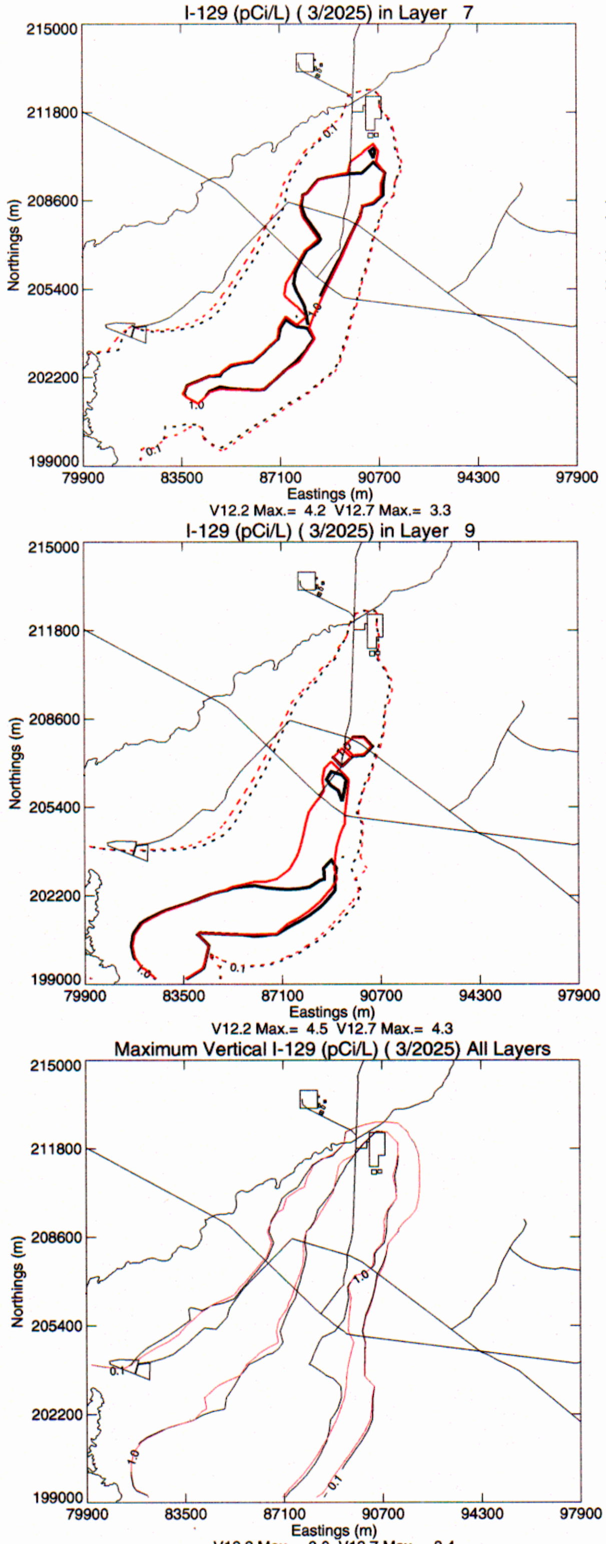

Figure 2-20 RI/BRA model I-129 concentrations, TETRAD version 12.2 (black) vs. 12.7 (red) for layers 7-10 in 3/2025.

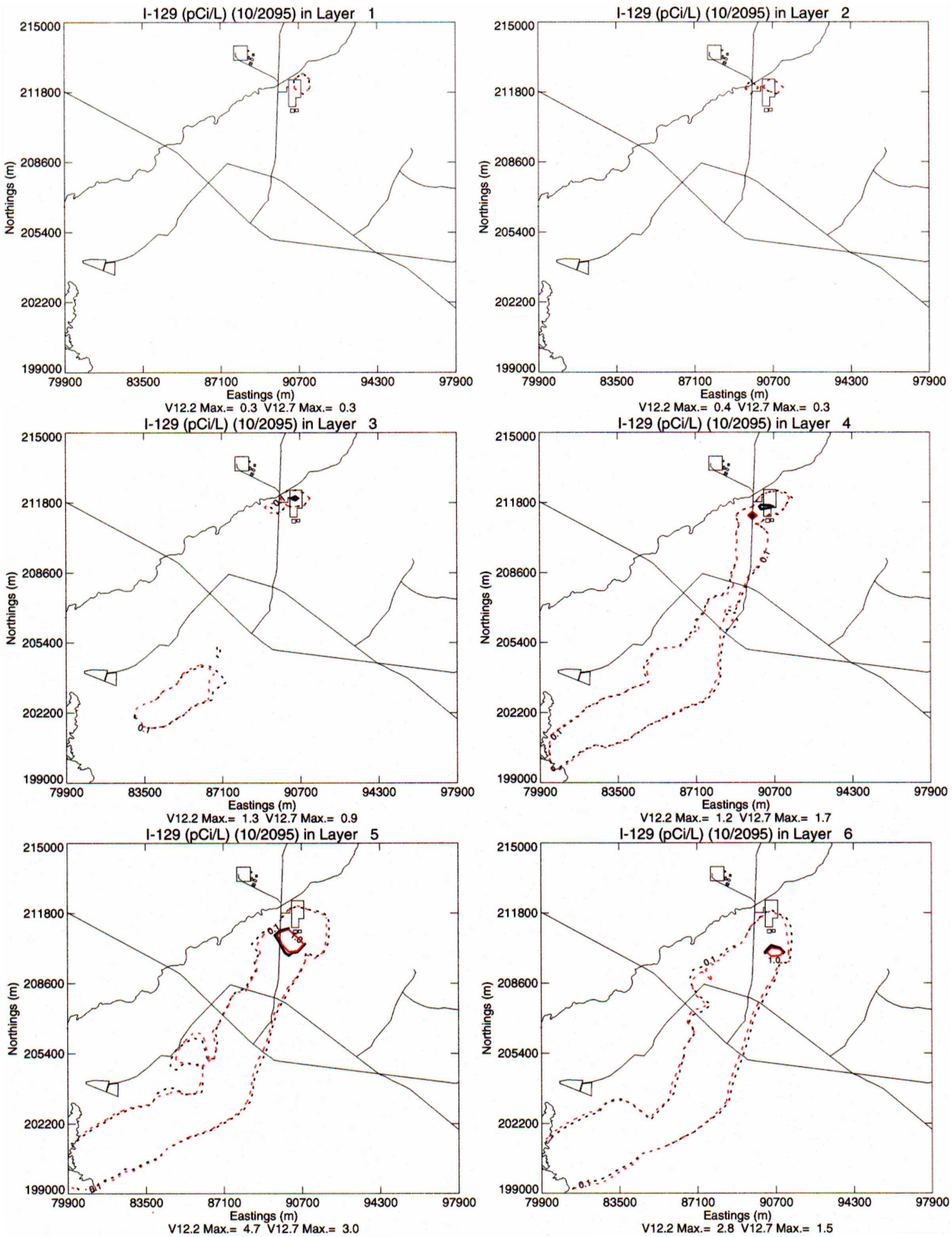

Figure 2-21 RI/BRA model I-129 concentrations, TETRAD version 12.2 (black) vs. 12.7 (red) for layers 1-6 in 10/2095.

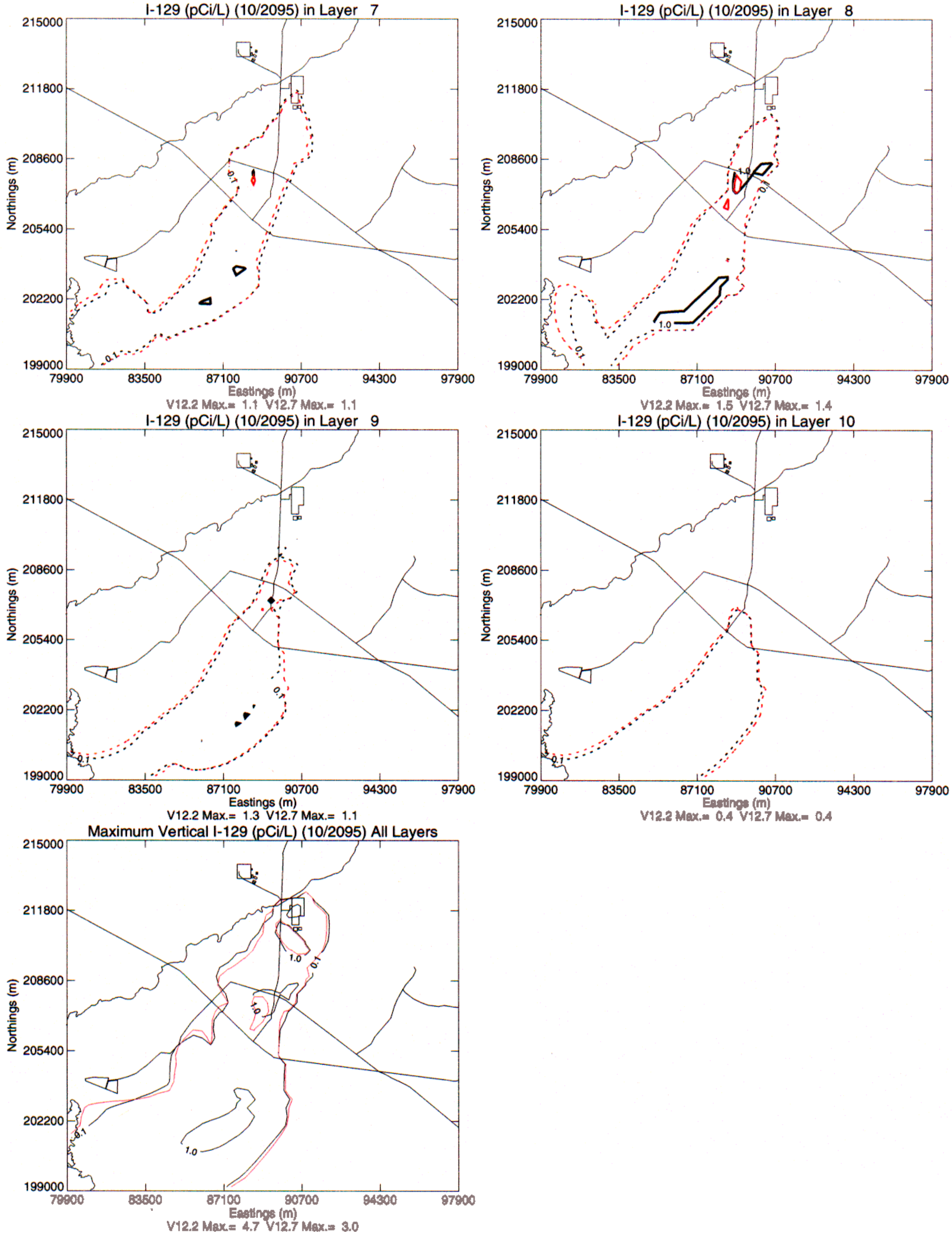

Figure 2-22 RI/BRA model I-129 concentrations, TETRAD version 12.2 (black) vs. 12.7 (red) for layers 7-10 in 10/2095.

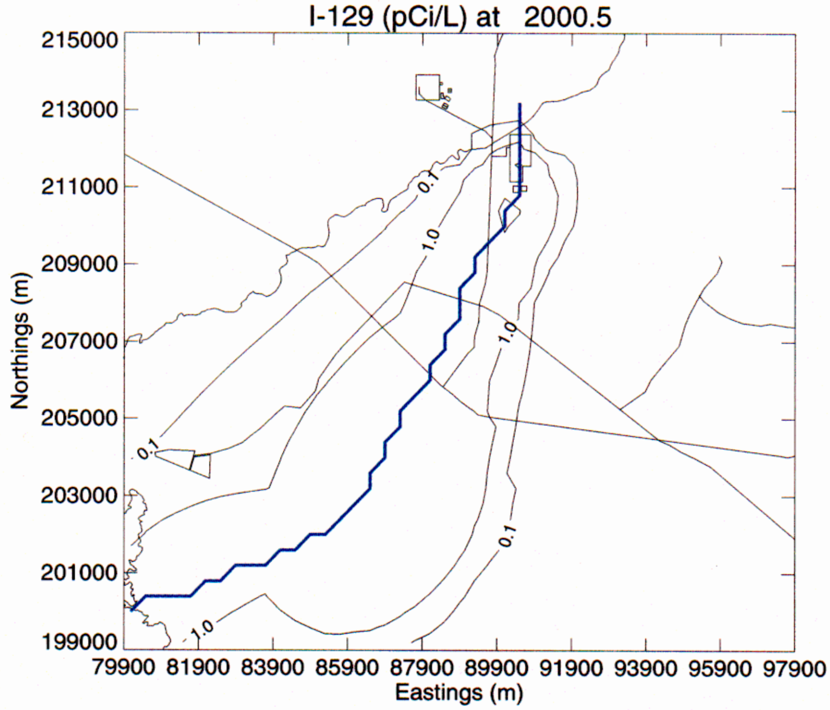

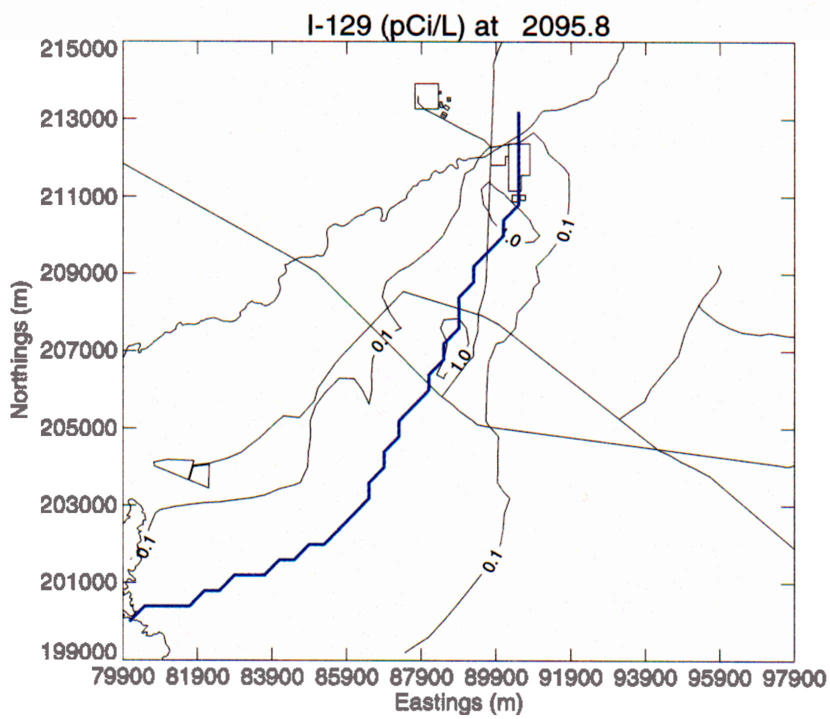

Figure 2-23 RI/BRA model maximum I-129 concentrations in 2000 and 2095 with plume axis (blue).

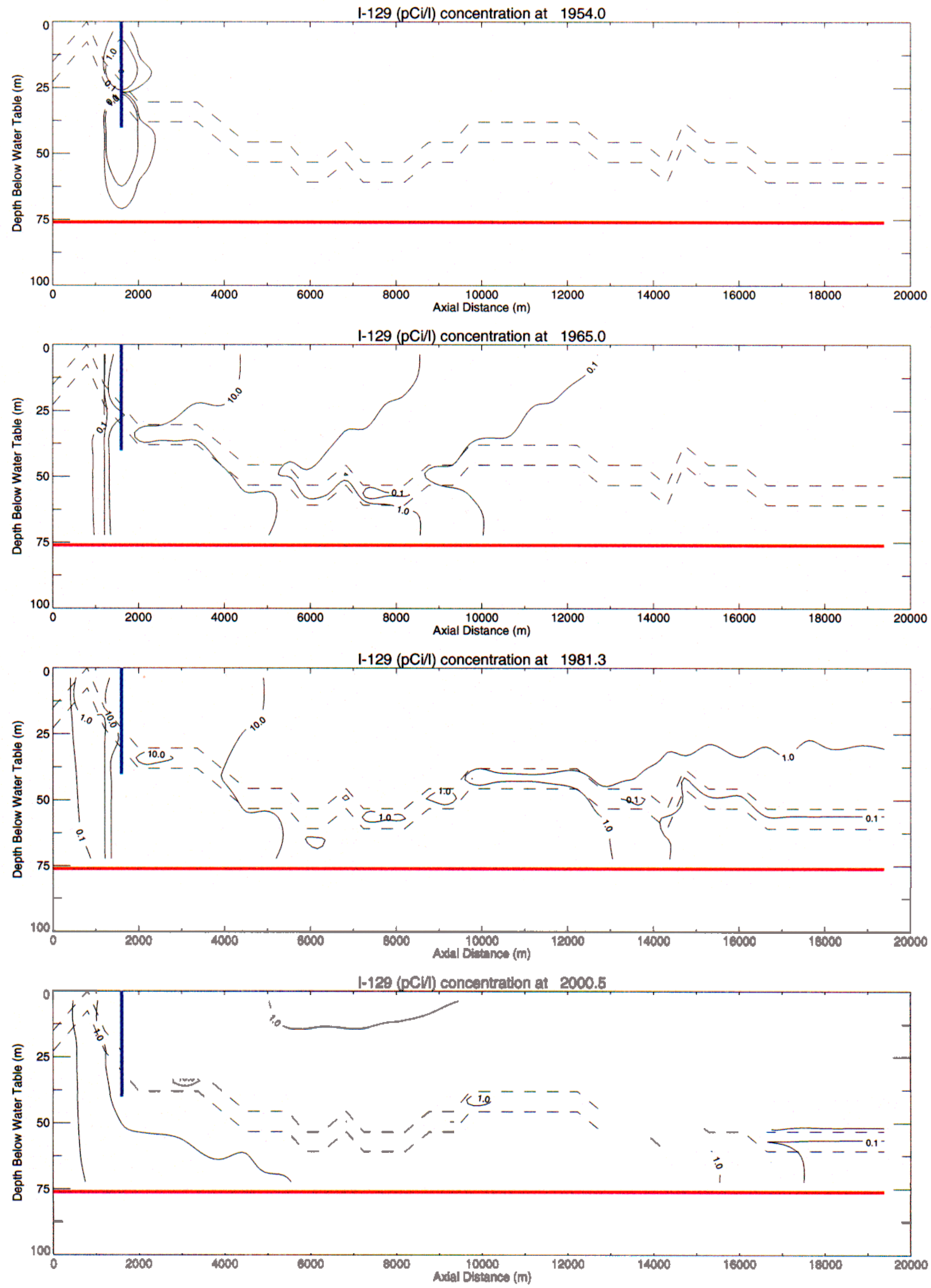

Figure 2-24 RI/BRA model plume axis vertical I-129 concentrations in 1954, 1965, 1981, and 2000 (the injection well is blue, the model bottom is red, and the long dashed black line represents the interbed).

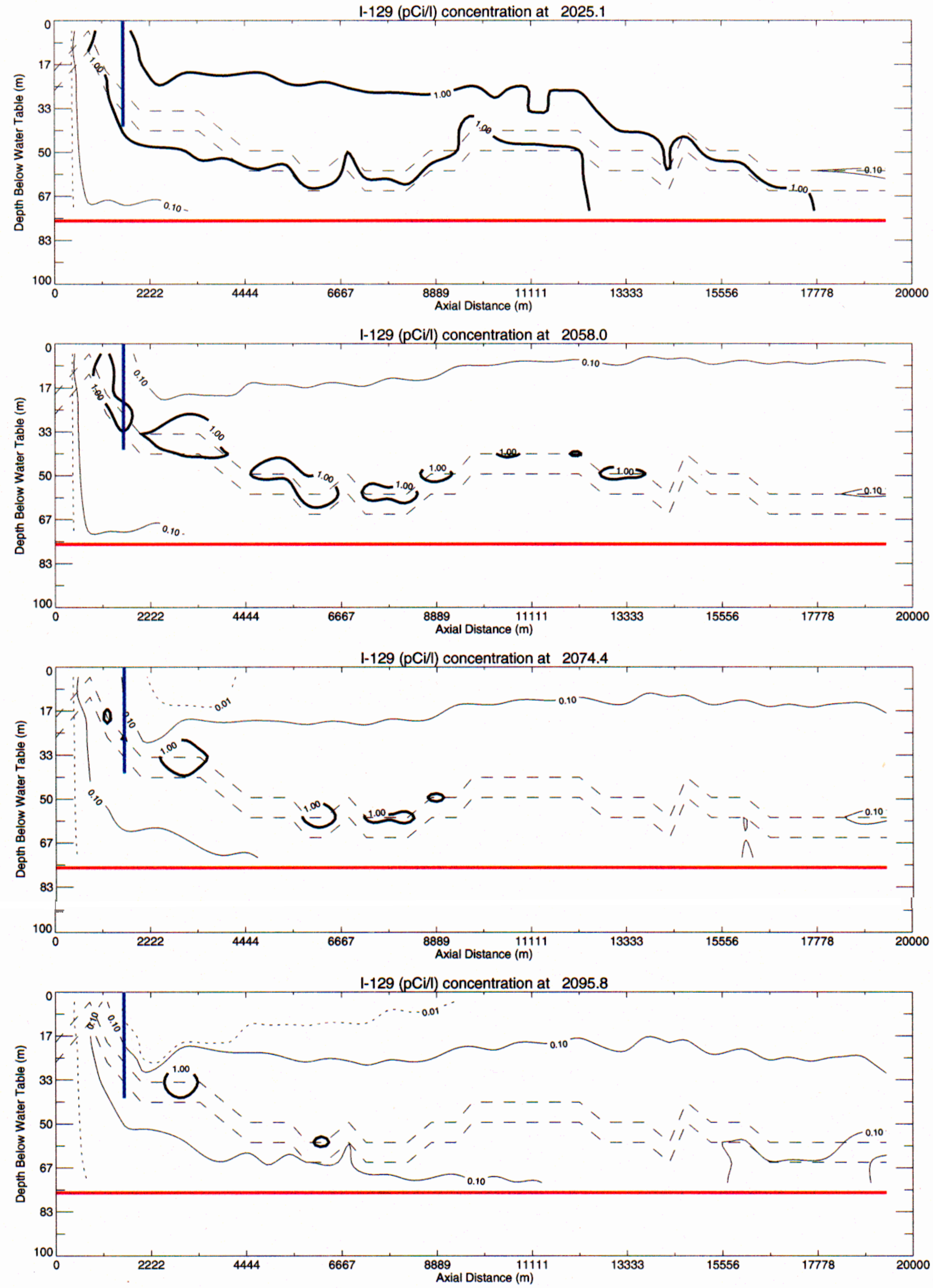

Figure 2-25 RI/BRA model plume axis vertical I-129 concentrations in 2025, 2058, 2074, and 2095 (the injection well is blue, the model bottom is red, and the long dashed black line represents the interbed).